The 15th International Conference on Advanced Robotics
Tallinn University of Technology
Tallinn, Estonia, June 20-23, 2011

Formation Control of Unicycle Robots Using the Virtual Structure Approach

Anna Sadowska, Henri Huijberts, Dragan Kostić, Nathan van de Wouw, Henk Nijmeijer

Abstract— **This paper addresses the problem of formation control of groups of unicycle robots with possibly time–varying formation shapes. To solve the problem, we propose two simple distributed formation control algorithms based on the virtual structure approach. We prove exponential convergence of error variables to the origin and illustrate the behavior of a group of robots under the formation control algorithm in simulations and experiments.**

I. Introduction

In recent years, the problem of synchronous control of multiple mobile robots has been the focus of attention of numerous researchers worldwide. In control theory, this problem is called a formation control problem or a coordination control problem, as the objective is to steer all robots in the formation in a coordinated fashion, see [13] and references therein. This in particular means that robots in the formation are required to create a given geometry of the formation while the group as a whole follows a desired trajectory. An alternative approach is what is referred to in the literature as cooperative path following [6] where path following as opposed trajectory tracking of robots in the formation is considered.

One approach to solve the formation control problem is the leader–follower approach, where one considers two types of robots in the formation: leaders and followers, see e.g. [3], [14]. The leaders are controlled independently, while the motion of the followers depends on the leaders associated with them. An important advantage of the leader–follower control scheme is its mathematical simplicity. However, due to the existence of group leaders, the whole formation may fail to execute its task if one of the leaders fails.

Another approach is the virtual structure approach in which in a certain sense the behavior of the formation is summarized in that of a so-called virtual structure. The virtual structure is to track a given desired trajectory. Then, knowing the desired behavior of the virtual structure, this behavior is converted to that of individual robots by imposing a certain formation shape. Therefore, in comparison to the leader-follower approach, it may be argued that the virtual structure approach allows for a greater deal of robustness as it does not depend critically on a single real (as opposed to virtual) unit. Examples of virtual structure algorithms are presented in, among others, [4], [9], [17].

A. Sadowska and H. Huijberts are with the School of Engineering and Materials Science, Queen Mary University of London; (e-mail: {a.d.sadowska, h.j.c.huijberts}@qmul.ac.uk); D. Kostić, N. van de Wouw and H. Nijmeijer are with the Demaprtment of Mechanical Engineering, Eindhoven University of Technology; (e-mail: {d.kostic, n.v.d.wouw, h.nijmeijer}@tue.nl).

A different type of division classifies formation control algorithms into those requiring either a global or a local communication network. In algorithms employing a global communication network, see e.g. [9], [17], all robots in the formation need to communicate with all remaining robots, which results in a burden of high communication cost. On the other hand, in formation control algorithms incorporating a local distributed communication network, robots in the formation do not need to exchange information with all remaining robots but instead they communicate with robots in their communication neighborhood only, see [5], [11].

To solve the formation control problem, we propose in this paper a distributed formation control algorithm, based upon the virtual structure approach and motivated by the results in [17]. Note that in [17] robots need to communicate with all other robots in the formation. Moreover, the algorithm [17] is nonlinear in terms of some of the error variables and only provides local convergence of the error variables to zero. In addition, in [17] the analysis of the formation control algorithm is rather limited in that only the case of two robots in the formation is given. In comparison with [17], the communication network considered in our paper is distributed. This means that each robot can only communicate locally with its neighbours. Furthermore, our results hold globally and the case of an arbitrary number of robots in the formation is studied, and the control algorithm is linear. In addition, we extend our main result to a dynamic formation control algorithm that takes into consideration mobile robots' dynamic properties such as mass or moment of inertia.

The outline of this paper is as follows. In Section II we formulate the formation control problem that is further solved in Section III, where we give our main results. In particular, in Subsection III-A we introduce the kinematic control law and in Subsection III-B we propose the dynamic formation control law. In Section IV we present a numerical and experimental study, and our conclusions are contained in Section V.

II. Problem Statement

In this section we formulate the formation control problem that is studied in this paper. We consider a formation consisting of n identical unicycle mobile robots with a nonholonomic no-side-slip constraint $\dot{x}\sin\theta - \dot{y}\cos\theta = 0$, where the state vector $q = (x, y, \theta)$ represents position (x, y) and orientation θ. Hence, motion of each robot in the group is given by ([2])

$$\dot{x}_i = v_i \cos\theta_i, \quad \dot{y}_i = v_i \sin\theta_i, \quad \dot{\theta}_i = \omega_i, \qquad (1)$$

978-1-4577-1159-6/11/$26.00 ©2011 IEEE

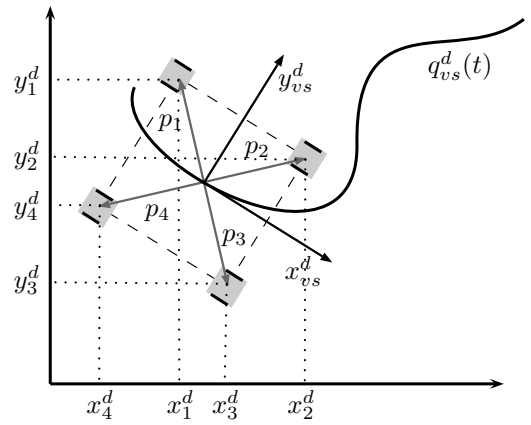

Fig. 1. Desired positions of robots in the formation with respect to the virtual structure's position and a given formation shape.

where $u_i = (v_i, \omega_i)^T$ is the control input of the i^{th} robot with v_i the forward velocity and ω_i the angular velocity, (x_i, y_i) are Cartesian coordinates of the robot and θ_i is its orientation.

Following the virtual structure approach, an additional virtual robot with identical kinematics (1) as for all ordinary robots in the group is introduced. This virtual robot is placed in the virtual center of the formation. Note that the virtual center does not need to be an actual geometric centroid of the formation but may be any point considered as central for a particular application. Based upon the position and orientation of the virtual center, desired positions of robots in the formation are given with the aid of possibly time varying bounded vectors $p_i(t) = (p_{xi}(t), p_{yi}(t))^T$ given with respect to the local coordinate system associated with the virtual robot that is in accordance to its orientation, see Fig. 1. Assume that vectors $\dot{p}_i(t)$ for all i are bounded.

For the formation control problem to be solved, we require the following set of equalities to hold asymptotically

$$\begin{pmatrix} x_i(t) \\ y_i(t) \end{pmatrix} - \begin{pmatrix} x_i^d(t) \\ y_i^d(t) \end{pmatrix} = \begin{pmatrix} 0 \\ 0 \end{pmatrix}, \qquad i = 1, \ldots, n, \quad (2)$$

in which $x_i^d(t)$ and $y_i^d(t)$ are calculated according to

$$\begin{aligned} x_i^d &= x_{vs}^d + p_{xi}\cos\theta_{vs}^d - p_{yi}\sin\theta_{vs}^d \\ y_i^d &= y_{vs}^d + p_{xi}\sin\theta_{vs}^d + p_{yi}\cos\theta_{vs}^d, \end{aligned} \quad (3)$$

where $x_{vs}^d(t)$ and $y_{vs}^d(t)$ define the desired trajectory of the virtual structure. Furthermore, θ_{vs}^d and θ_i^d follow from the no-side-slip constraint and $\left(x_{vs}^d, y_{vs}^d\right)$ or $\left(x_i^d, y_i^d\right)$ respectively. Let v_{vs}^d and ω_{vs}^d be desired forward and angular velocities respectively, associated with the desired trajectory $(x_{vs}^d(t), y_{vs}^d(t))$ of the virtual structure. Assume that v_{vs}^d and ω_{vs}^d are bounded. By differentiating x_i^d and y_i^d in time and comparing the result with the desired kinematics of robot i of the same form as (1), one obtains desired velocities for each individual robot:

$$v_i^d = \sqrt{(\dot{x}_i^d)^2 + (\dot{y}_i^d)^2}, \qquad \omega_i^d = \frac{\ddot{y}_i^d \dot{x}_i^d - \ddot{x}_i^d \dot{y}_i^d}{(\dot{x}_i^d)^2 + (\dot{y}_i^d)^2}. \quad (4)$$

Then, following [7], the error variables of robot i are defined by

$$\begin{pmatrix} x_i^e \\ y_i^e \\ \theta_i^e \end{pmatrix} = \begin{bmatrix} \cos\theta_i & \sin\theta_i & 0 \\ -\sin\theta_i & \cos\theta_i & 0 \\ 0 & 0 & 1 \end{bmatrix} \begin{pmatrix} x_i^d - x_i \\ y_i^d - y_i \\ \theta_i^d - \theta_i \end{pmatrix}, \quad (5)$$

and their time derivatives can be shown to be given by

$$\begin{aligned} \dot{x}_i^e &= \omega_i y_i^e - v_i + v_i^d \cos\theta_i^e \\ \dot{y}_i^e &= -\omega_i x_i^e + v_i^d \sin\theta_i^e \qquad (i = 1, \ldots, n) \\ \dot{\theta}_i^e &= \omega_i^d - \omega_i. \end{aligned} \quad (6)$$

Therefore, the formation control problem may be stated as the requirement to render the error dynamics (6) globally asymptotically stable.

III. Control Algorithms

In this section, we propose two formation control algorithms, one of which is a kinematic control algorithm, see Theorem 3.1 and the other one is a dynamic formation control algorithm, see Theorem 3.2.

Both formation control algorithms employ a modified version of the control algorithm proposed originally for a single nonholonomic system by Panteley *et al* [12]. The augmentation that is crucial for a formation control algorithm involves including a robot's neighbors' actual performance. Therefore, for the i^{th} robot we introduce additional mutual coupling terms $x_i^e - x_j^e$, $y_i^e - y_j^e$ and $\theta_i^e - \theta_j^e$ for each robot $j \in N_i$. Here N_i denotes a set of indices of neighbors of robot $i \in \{1, \ldots, n\}$ that is $N_i = \left\{j \in \{1, \ldots, n\} \,\middle|\, j \neq i \text{ and } a_{ij} \neq 0\right\}$, in which a_{ij} is the (i, j)-th element of the adjacency matrix of the corresponding communication graph.

A. Kinematic control law

In this section we present a distributed kinematic control algorithm. Based on the discussion above, we propose the following controller

$$\begin{aligned} v_i &= v_i^d + c_i^x x_i^e - c_i^y \omega_i^d y_i^e \\ &\quad + \sum_{j \in N_i} \widetilde{c}_{ij}^x (x_i^e - x_j^e) - \sum_{j \in N_i} \widetilde{c}_{ij}^y \omega_i^d (y_i^e - y_j^e), \\ \omega_i &= \omega_i^d + c_i^\theta \theta_i^e + \sum_{j \in N_i} \widetilde{c}_{ij}^\theta (\theta_i^e - \theta_j^e), \end{aligned} \quad (7)$$

where the control parameters are to be defined below. Note that the original tracking algorithm for a single mobile robot proposed by Panteley *et al* [12] can be retrieved by setting all coupling gains to zero, i.e. $\widetilde{c}_{ij}^x = 0$, $\widetilde{c}_{ij}^y = 0$, $\widetilde{c}_{ij}^\theta = 0$. In the case of formation control, these mutual coupling gains are crucial for robots in the formation to be aware of their neighbors' states. The importance of the mutual coupling terms becomes apparent if some of the robots in the formation are subject to a perturbation. This will be illustrated in Section IV.

In the following theorem, we examine when the formation control problem as defined in the Introduction is solved using the control law given in (7).

Theorem 3.1: Consider a group of n nonholonomic mobile robots (1), a desired trajectory of the virtual structure of the formation $(x_{vs}^d(t), y_{vs}^d(t))$, a desired formation shape given by vectors $p_i(t)$ and associated desired trajectories of robots in the formation (3) together with desired forward and angular velocities (4). Let the control law be defined in (7) in which c_i^x, c_i^y, c_i^θ, $\widetilde{c}_{ij}^x$,$\widetilde{c}_{ij}^y$, $\widetilde{c}_{ij}^\theta$ are positive parameters such that $\widetilde{c}_{ij}^x = \widetilde{c}_{ji}^x$ and $\widetilde{c}_{ij}^y = \widetilde{c}_{ji}^y$ and $\widetilde{c}_{ij}^\nu \neq 0$ iff $j \in N_i$ where $\nu = \{x, y, \theta\}$. Assume that $\bar{\Omega}^d(t) = \mathrm{col}(\omega_1^d(t), \ldots, \omega_N^d(t))$ satisfies the persistence of excitation condition ([8]) and $v_i^d(t)$ is nonzero, for all t. Then the closed–loop error dynamics (6) and (7) have a globally $\mathcal{K}$–exponentially stable ([16]) equilibrium point and hence the control law (7) solves the formation control problem.

Proof: Application of the control law (7) yields the following closed–loop error dynamics of the overall formation

$$\underbrace{\begin{pmatrix}\dot{X}^e\\ \dot{Y}^e\end{pmatrix} = \begin{bmatrix}-\mathbf{C}^x & \mathbf{\Omega}^d\Big(\mathbf{C}^y + \mathbf{I}\Big)\\ -\mathbf{\Omega}^d & \mathbf{0}\end{bmatrix}\begin{pmatrix}X^e\\ Y^e\end{pmatrix}}_{\dot{z}_1 = f_1(t, z_1)} + \underbrace{\begin{bmatrix}\bar{\mathbf{Y}}^e\mathbf{C}^\theta + \mathbf{V}^d\mathbf{\Theta}_{\cos}\\ -\bar{\mathbf{X}}\mathbf{C}^\theta + \mathbf{V}^d\mathbf{\Theta}_{\sin}\end{bmatrix}\Theta^e}_{g(t, z_1, z_2)}$$
$$\underbrace{\dot{\Theta}^e = -\mathbf{C}^\theta\Theta^e}_{\dot{z}_2 = f_2(z_2)} \tag{8}$$

where $X^e = \mathrm{col}(x_1^e, \ldots, x_n^e)$, $Y^e = \mathrm{col}(y_1^e, \ldots, y_n^e)$, $\bar{\mathbf{X}}^e = \mathrm{diag}(x_1^e, \ldots, x_n^e)$, $\bar{\mathbf{Y}}^e = \mathrm{diag}(y_1^e, \ldots, y_n^e)$, $\mathbf{\Omega}^d = \mathrm{diag}(\omega_1^d, \ldots, \omega_n^d)$, $\mathbf{V}^d = \mathrm{diag}(v_1^d, \ldots, v_n^d)$, $\mathbf{\Theta}_{\cos} = \mathrm{diag}\left(\frac{\cos\theta_1^e - 1}{\theta_1^e}, \ldots, \frac{\cos\theta_n^e - 1}{\theta_n^e}\right)$ and $\mathbf{\Theta}_{\sin} = \mathrm{diag}\left(\frac{\sin\theta_1^e}{\theta_1^e}, \ldots, \frac{\sin\theta_n^e}{\theta_n^e}\right)$. Note that $\frac{\sin\theta_i^e}{\theta_i^e}$ and $\frac{\cos\theta_i^e - 1}{\theta_i^e}$ are smooth if their definition is extended to $\theta_i^e = 0$ in the standard way. The remaining matrices $\mathbf{C}^\nu$ for $\nu = \{x, y, \theta\}$ in (8) are:

$$\mathbf{C}^\nu = \begin{bmatrix} d_1 & -\widetilde{c}_{12}^\nu & \ldots & -\widetilde{c}_{1n}^\nu \\ \vdots & \ddots & \ddots & \vdots \\ -\widetilde{c}_{n-11}^\nu & \ddots & d_{n-1} & -\widetilde{c}_{n-1n}^\nu \\ -\widetilde{c}_{n1}^\nu & -\widetilde{c}_{n2}^\nu & \ldots & d_n \end{bmatrix}, \tag{9}$$

in which $d_i = c_i^\nu + \sum_{j\in N_i}\widetilde{c}_{ij}^\nu$ and for $i \neq j$, we have $\mathbf{C}_{ij}^\nu \neq 0$ iff $j \in N_i$. Moreover, using the Geršgorin disc theorem, we can show that all eigenvalues of matrices $\mathbf{C}^\nu$ for $\nu = \{x, y, \theta\}$ lie in the open right-half plane of the complex plane. Thus, since $\mathbf{C}^x$ and $\mathbf{C}^y$ are symmetric, it is apparent that $\mathbf{C}^x$ and $\mathbf{C}^y$ are positive definite.

Clearly, system (8) has the cascade form as in [12]. Thus, if the assumptions of [12, Lemma 8] (cf. [1]) hold, the origin of the overall system is globally $\mathcal{K}$-exponentially stable. They can be verified as follows.

Consider the first stage of the cascade, i.e. $\dot{z}_1 = f_1(t, z_1)$ in which $z_1 = \mathrm{col}(z_{11}, z_{12})$. Let

$$V(z_{11}, z_{12}) = \frac{1}{2}(z_{11}^T z_{11} + z_{12}^T(\mathbf{I} + \mathbf{C}^y)z_{12}). \tag{10}$$

Its derivative along solutions of $\dot{z}_1 = f_1(t, z_1)$ satisfies

$$\dot{V}(z_{11}, z_{12}) = -z_{11}^T\mathbf{C}^x z_{11} \leq 0. \tag{11}$$

Moreover, analysis of the observability condition, similarly to the developments in [8, Appendix A.20], leads us to the conclusion that for ω_i^d being persistently exciting, the observability Gramian of the pair $(A(t), C)$ indeed is a uniformly positive definite matrix, where $A(t)$ is the system matrix of the linear system $\dot{z}_1 = f_1(t, z_1)$ and C is such that $z_{11}^T\mathbf{C}^x z_{11} = z_1^T C^T C z_1$. Thus, from [8, Theorem 4.5], $z_1 = 0$ is a globally exponentially stable equilibrium of $\dot{z}_1 = f_1(t, z_1)$.

Furthermore, as mentioned earlier $\mathbf{C}^\theta$ has all eigenvalues in the open right–half plane. Therefore the equilibrium $z_2 = 0$ of $\dot{z}_2 = f_2(z_2)$ is globally exponentially stable.

Next, notice that $\|g(t, z_1, z_2)\|_F \leq 2nv^* + \|\mathbf{C}^\theta\|\|z_1\|$, where $v_i^* = \sup\{|v_i^d(t)| \mid t \geq 0\}$ and $v^* = \max\{v_i^* \mid i = 1, \ldots, n\}$ and $\|\cdot\|_F$ denotes the Frobenius norm, see [8]. Note that boundedness of v_i^d is implied by boundedness of v_{vs}^d, ω_{vs}^d, p_i and $\dot{p}_i$. Therefore it follows from [12, Lemma 8] (cf. [1]), that the origin $(z_1, z_2) = (0, 0)$ of the cascade system (8) is globally $\mathcal{K}$–exponentially stable. Thus, the control law (7) solves the formation control problem studied in this paper.

This completes the proof. ∎

B. Dynamic formation control law

In this section we consider a distributed dynamic control algorithm based on a simple dynamic model of a mobile robot ([12]) given by (1) and

$$\dot{v}_i = \frac{F_i}{m_i}, \quad \dot{\omega}_i = \frac{\tau_i}{J_i}, \tag{12}$$

in which m_i denotes the mass of the i^{th} robot, J_i is its moment of inertia around the vertical axis passing through its center of mass and the control inputs F_i and τ_i denote force and torque, applied to robot i, respectively.

The dynamic formation control algorithm is an extension of the kinematic control law presented in the previous subsection and is motivated by the developments in [12]. Based on the control law defined in Theorem 3.1, we define desired forward and angular velocities $\bar{v}_i$ and $\bar{\omega}_i$ to be equal to the desired inputs given in (7). Also, we define additional error variables by $v_i^e = v_i - \bar{v}_i$ and $\omega_i^e = \omega_i - \bar{\omega}_i$. Consequently, the following error dynamics for the overall formation is obtained

$$\begin{pmatrix}\dot{X}^e\\ \dot{Y}^e\\ \dot{V}^e\end{pmatrix} = \begin{bmatrix}-\mathbf{C}^x & \mathbf{\Omega}^d\Big(\mathbf{C}^y + \mathbf{I}\Big) & -\mathbf{I}\\ -\mathbf{\Omega}^d & \mathbf{0} & \mathbf{0}\\ \mathbf{0} & \mathbf{0} & \mathbf{0}\end{bmatrix}\begin{pmatrix}X^e\\ Y^e\\ V^e\end{pmatrix} + \begin{pmatrix}\mathbf{0}\\ \mathbf{0}\\ \mathbf{I}\end{pmatrix}\Big(\mathbf{M}^{-1}F - \dot{\bar{V}}\Big) + \begin{bmatrix}\bar{\mathbf{Y}}^e\mathbf{C}^\theta + \mathbf{V}^d\mathbf{\Theta}_{\cos} & \bar{\mathbf{Y}}^e\\ -\bar{\mathbf{X}}^e\mathbf{C}^\theta + \mathbf{V}^d\mathbf{\Theta}_{\sin} & -\bar{\mathbf{X}}^e\\ \mathbf{0} & \mathbf{0}\end{bmatrix}\begin{pmatrix}\Theta^e\\ \Omega^e\end{pmatrix} \tag{13}$$

$$\begin{pmatrix}\dot{\Theta}^e\\ \dot{\Omega}^e\end{pmatrix}=\begin{bmatrix}-\mathbf{C}^\theta & -\mathbf{I}\\ \mathbf{0} & \mathbf{0}\end{bmatrix}\begin{pmatrix}\Theta^e\\ \Omega^e\end{pmatrix}+\begin{pmatrix}\mathbf{0}\\ \mathbf{I}\end{pmatrix}\left(\mathbf{J}^{-1}T-\dot{\bar{\Omega}}\right),$$

where $V^e = \mathrm{col}(v_1^e,\ldots,v_n^e)$, $\Omega^e = \mathrm{col}(\omega_1^e,\ldots,\omega_n^e)$, $\mathbf{M} = \mathrm{diag}(m_1,\ldots,m_n)$, $\mathbf{J} = \mathrm{diag}(J_1,\ldots,J_n)$, $F = \mathrm{col}(F_1,\ldots,F_n)$, $T = \mathrm{col}(\tau_1,\ldots,\tau_n)$, $\dot{\bar{V}} = \mathrm{col}(\dot{\bar{v}}_1,\ldots,\dot{\bar{v}}_n)$ and $\dot{\bar{\Omega}} = \mathrm{col}(\dot{\bar{\omega}}_1,\ldots,\dot{\bar{\omega}}_n)$. Moreover, the constant matrices $\mathbf{C}^x$, $\mathbf{C}^y$ and $\mathbf{C}^\theta$ are defined in (9). The control design, as motivated by [12], now relies on defining the control inputs F and T for the whole formation in such a way, that the resultant closed–loop error dynamics have a cascade structure as in [1], [12] and are globally $\mathcal{K}$–exponentially stable.

To this end, we propose the following control input

$$F=\mathbf{M}\left(\dot{\bar{V}}+\mathbf{C}^{vx}X^e-\mathbf{C}^{vv}V^e\right),\quad T=\mathbf{J}\left(\dot{\bar{\Omega}}-\mathbf{C}^{\omega}\Omega^e\right),\tag{14}$$

where $\mathbf{C}^{vx}=\mathrm{diag}(c_1^{vx},\ldots,c_n^{vx})$, $\mathbf{C}^{vv}=\mathrm{diag}(c_1^{vv},\ldots,c_n^{vv})$ and $\mathbf{C}^{\omega}=\mathrm{diag}(c_1^{\omega},\ldots,c_n^{\omega})$ are positive definite matrices. It will be shown in the following theorem that indeed application of (14) to the formation of mobile robots with the open loop error dynamics (13) globally $\mathcal{K}$–exponentially stabilizes this system.

Theorem 3.2: Consider n unicycle mobile robots satisfying (1, 12), desired trajectories of robots in the formation (3) and desired forward and angular velocities of the robots (4). Consider the control law defined in (14), where c_i^{vx}, c_i^{vv}, c_i^{ω} are positive parameters and additional kinematic control parameters in are given in Theorem 3.1. Assume that $\bar{\Omega}^d(t)=\mathrm{col}(\omega_1^d(t),\ldots,\omega_N^d(t))$ satisfies the persistence of excitation condition, and $v_i^d(t)$ is nonzero, $i=1,\ldots,n$. Then, the origin of the closed–loop error dynamics (13)–(14) is globally $\mathcal{K}$–exponentially stable and, hence, the formation control problem is solved.

Proof: The proof can be established by essentially following the same lines as the proof of Theorem 3.1. It is omitted here due to space limitation. The interested reader is referred to [15]. ∎

Remark 3.3: Theorems 3.1 and 3.2 give only weak conditions regarding the control parameters. Therefore, one can choose the control parameters in a way that is desirable for a specific application. In particular, to focus on tracking of individual robots' trajectories, the self-tracking gains c_i^x, c_i^y, c_i^θ should dominate the mutual coupling gains $\widetilde{c}_{ij}^x$, $\widetilde{c}_{ij}^y$, $\widetilde{c}_{ij}^\theta$. Moreover, also dynamic tracking parameters c_i^{vx}, c_i^{vv}, c_i^{ω} correspond to pure trajectory tracking. On the other hand, when keeping formation is the major objective, the mutual coupling gains $\widetilde{c}_{ij}^x$, $\widetilde{c}_{ij}^y$ and $\widetilde{c}_{ij}^\theta$ ought to dominate the self-tracking gains c_i^x, c_i^y, c_i^θ.

IV. Experimental and Simulation study

In this section, we present experimental and numerical results of a formation of three robots with two different communication structures: a connected one, as illustrated in Fig. 2(a), and a disconnected one, as illustrated in Fig. 2(b) or a fully disconnected where there are no communication links. For the kinematic algorithm we give experimental results while for the dynamic formation controller simulation results are given.

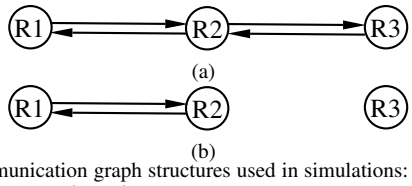

Fig. 2. Communication graph structures used in simulations: (a) connected graph (b) disconnected graph.

TABLE I

List of control parameters used in experiments in Section IV-A.

$c_i^x = 1\ \frac{1}{\mathrm{s}}$	$c_i^y = 30$	$c_i^\theta = 0.5\ \frac{1}{\mathrm{s}}$
$\widetilde{c}_{ij}^x = 2.5\ \frac{1}{\mathrm{s}}$	$\widetilde{c}_{ij}^y = 30$	$\widetilde{c}_{ij}^\theta = 0.1\ \frac{1}{\mathrm{s}}$

For both algorithms we consider a formation geometry maintenance index defined as

$$I(t)=\sum_{i=1}^{3}\sum_{\substack{j=1\\ j\neq i}}^{3}\left(\|r_i(t)-r_j(t)\|-\|p_i(t)-p_j(t)\|\right)^2,\tag{15}$$

in which $r_i(t)=\mathrm{col}(x_i(t),y_i(t))$ denote a robot's actual position in the inertial frame and $p_i(t)$ a robot's desired position in the formation. The index (15) shows discrepancy between actual formation shape and the desired one.

A. Kinematic formation control algorithm

In this section we illustrate the behavior of a mobile robot formation under the influence of the kinematic control law given in Theorem 3.1 based on experiments. The experiments were performed at Eindhoven University of Technology using three e-puck mobile robots [10]. The experimental set-up consists of a 2.2 by 3.2 m arena and a camera based localization system. More details can be found in [15].

The control parameters employed in the experiments are summarized in Table I. Moreover, the desired virtual structure's trajectory is given by

$$x_{vs}^d(t)=0.05t-1.2,\quad y_{vs}^d(t)=0.1\cos(0.3t)+0.025t-0.7,\tag{16}$$

where x_{vs}^d and y_{vs}^d are in meters and t is in seconds.

The desired formation shape is an equilateral triangle, where $p_1 = \left(-0.15,-\frac{0.15}{\sqrt{3}}\right)^T$ m, $p_2 = \left(0.15,-\frac{-0.15}{\sqrt{3}}\right)^T$ m and $p_3=\left(0,\frac{0.3}{\sqrt{3}}\right)^T$ m. Thus the sides of the triangle have a length of 0.3 m. During the experiment, we manually perturbed one of the robot after around 30 s to observe the behavior of the formation in the presence of perturbation.

The experimental results are presented in Fig. 3-5. In particular, in Fig. 3 we present the robots' paths in the case of completely uncoupled robots, where $\widetilde{c}_{ij}^x = 0$, $\widetilde{c}_{ij}^y = 0$ and $\widetilde{c}_{ij}^\theta = 0$. In turn, in Fig. 4, robots' paths in the plane are presented when the communication graph is connected according to the communication network shown in Fig. 2(a). It can be seen in the plots, that in both cases robots in the formation converge to the desired formation shape. Moreover, after the perturbation has occurred, the neighbors of the perturbed robot diverge from their desired trajectories

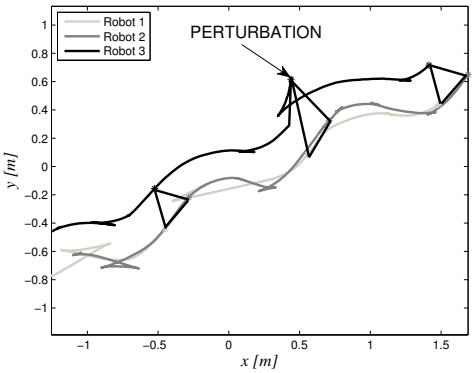

Fig. 3. Robot paths on the plane in the case of a disconnected communication graph and the kinematic control algorithm (7).

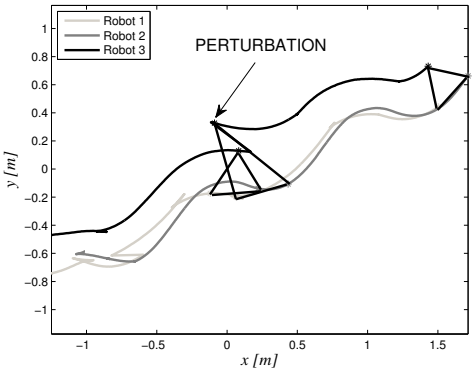

Fig. 4. Robot paths on the plane in the case of a connected communication graph and the kinematic control algorithm (7).

to preserve the formation shape. This is induced by the coupling terms added to the formation control algorithm. We can therefore confirm that these additional coupling terms in (7) enhance formation behavior of robots in the formation. Even more clearly the beneficial influence of allowing robots in the formation to exchange information with each other is visible in Fig. 5 which compares the formation geometry maintenance index (15) for a connected and a disconnected communication graph. Clearly, when the communication graph is connected, the index is smaller except for the perturbation peak. This is purely due to the fact that in experiments the displacement is done manually and therefore is not equal in the case of a connected and a disconnected communication graph. In fact, it is larger in the first instance which may be seen explicitly by comparing Fig. 3 and Fig. 4. Apart from the very moment of the perturbation, the formation geometry maintenance index is smaller. Moreover, despite the larger perturbation magnitude, the formation geometry maintenance index decreases faster in the case of a connected communication graph.

B. Dynamic formation control algorithm

In this section we present the simulation results for the dynamic formation control law given in Section III-B with control parameters given in Table II.

For both connected and disconnected communication networks (see Fig. 2), we allow for perturbations to appear to

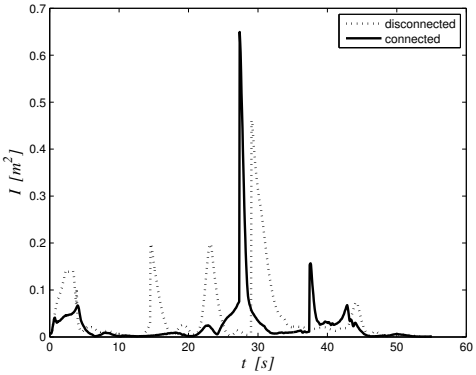

Fig. 5. Comparison between formation geometry maintenance index in the case of a connected and a disconnected communication graph.

TABLE II

LIST OF CONTROL PARAMETERS USED IN SIMULATIONS IN SECTION IV-B.

Robot 1	$c_1^x = 6$ $\widetilde{c}_{12}^x = 19$ $\widetilde{c}_{13}^x = 0$ $c_1^{vv} = 15$	$c_1^y = 4$ $\widetilde{c}_{12}^y = 15$ $\widetilde{c}_{13}^y = 0$ $c_1^{vx} = 15$	$c_1^\theta = 0.1$ $\widetilde{c}_{12}^\theta = 3$ $\widetilde{c}_{13}^\theta = 0$ $c_2^\omega = 15$
Robot 2	$c_2^x = 6$ $\widetilde{c}_{21}^x = 19$ $\widetilde{c}_{23}^x = 27$ $c_2^{vv} = 15$	$c_2^y = 1.5$ $\widetilde{c}_{21}^y = 15$ $\widetilde{c}_{23}^y = 15$ $c_2^{vx} = 15$	$c_2^\theta = 0.3$ $\widetilde{c}_{21}^\theta = 3$ $\widetilde{c}_{23}^\theta = 3$ $c_2^\omega = 15$
Robot 3	$c_3^x = 2$ $\widetilde{c}_{31}^x = 0$ $\widetilde{c}_{32}^x = 27$ $c_3^{vv} = 9$	$c_3^y = 3$ $\widetilde{c}_{31}^y = 0$ $\widetilde{c}_{32}^y = 15$ $c_3^{vx} = 9$	$c_3^\theta = 0.5$ $\widetilde{c}_{31}^\theta = 0$ $\widetilde{c}_{32}^\theta = 3$ $c_3^\omega = 15$

Robot 1 at time $t = 200$ when we displace this robot from its current position along $(\delta x, \delta y) = (15, -26)$.

We choose the desired trajectory of the formation's virtual structure as

$$\dot{x}_{vs}^d = 5\cos\theta_{vs}^d \quad \dot{y}_{vs}^d = 5\sin\theta_{vs}^d, \quad \dot{\theta}_{vs}^d = 0.2\sin t \qquad (17)$$

in which $x_{vs}^d(0) = 0$, $y_{vs}^d(0) = 0$ and $\theta_{vs}^d(0) = 0$. Moreover, initial conditions of robots in the formation are given by $q_1(0) = \left(-23.56, 4.01, -\frac{\pi}{3}\right)$, $q_2(0) = (5, 1.23, -\pi)$ and $q_3(0) = \left(12, 15.55, \frac{\pi}{2}\right)$. Furthermore, the desired formation shape is defined via $p_1 = \left(-10, -\frac{10\sqrt{3}}{3}\right)^T$, $p_2 = \left(10, -\frac{10\sqrt{3}}{3}\right)^T$ and $p_3 = \left(0, \frac{20\sqrt{3}}{3}\right)^T$ and again forms an equilateral triangle in which the length of the sides equals 20. All simulations are performed for the period of time $t \in [0, 300]$.

In Fig. 6 and 7, robot paths in the case of a connected and a disconnected communication graph are shown, respectively. It can be concluded that initially all robots converge to their desired position in the formation which changes when the perturbation occurs. Similarly as in the kinematic controller, we observe that only when communication graph is connected, all robots try to counteract the perturbation and maintain the desired formation shape. Accordingly, formation geometry maintenance index plotted in Fig. 8 converges to zero faster when the connectivity condition holds and moreover, the discrepancy between the desired and actual formation shape is smaller.

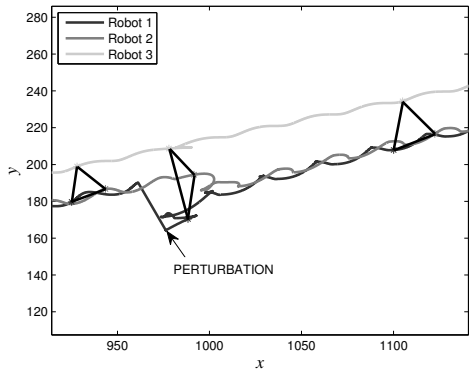

Fig. 6. Robot paths on the plane during the perturbation in the case of a connected communication graph and the dynamic control algorithm (14).

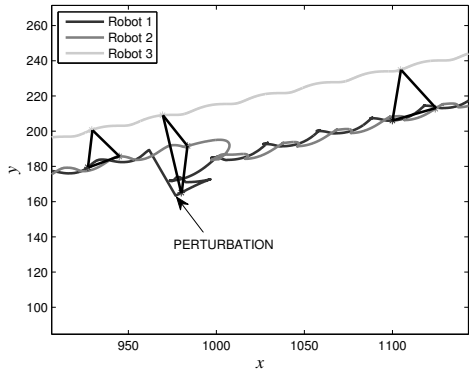

Fig. 7. Robot paths on the plane during the perturbation in the case of a disconnected communication graph and the dynamic control algorithm (14).

V. Conclusions

In this paper, we have considered the problem of formation control of unicycle robots with possibly time-varying desired formation shapes and proposed two control algorithms based on the virtual structure approach. Both of the algorithms are distributed and therefore, all robots plan their actions based upon local interactions between neighboring robots which is a considerable strength of our approach. The strengths of our results follow also, among others, from their simplicity in that the feedback terms introduced for the formation control are linear functions of the robot states. It also needs to be stressed that the results proposed in this paper hold globally. Furthermore, the weak condition of the persistence of excitation of the angular velocity of a desired trajectory to be tracked, allows for a broad range of practical applications.

It should also be mentioned that although we do not aim to provide any theoretical performance analysis of the formation control algorithms proposed in this paper, simulation and experimental results have shown a clear trend in that manner. In particular we have observed that if the communication graph of the formation is connected, the performance of the formation and more specifically sensitivity to perturbation is improved.

Our future work will include a more extensive theoretical analysis of the influence of the connectivity of the communication graph on formation behavior. Moreover, we also want to examine some practical issues of the formation control, i.e.

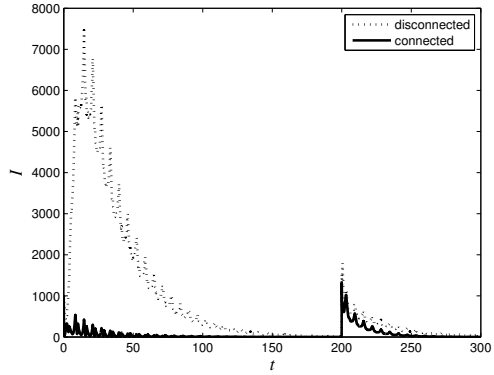

Fig. 8. Comparison between formation geometry maintenance index using the dynamic control algorithm for a connected and a disconnected communication graph.

a possibility of temporary communication failures, control inputs limits or lack of the fulfilment of the PE condition of the desired angular velocities.

References

[1] E. Aneke, "Control of underactuated mechanical systems," Ph.D. dissertation, Technische Universiteit Eindhoven, 2003.

[2] C. C. de Wit, G. Bastin, and B. Siciliano, Eds., *Theory of Robot Control*. Berlin, Heidelberg: Springer-Verlag New York, Inc., 1996.

[3] J. P. Desai, J. P. Ostrowski, and V. Kumar, "Modeling and control of formations of nonholonomic mobile robots," *IEEE Trans. Robot. Automat.*, vol. 17, no. 6, pp. 905–908, 2001.

[4] K. Do and J. Pan, "Nonlinear formation control of unicycle-type mobile robots," *Robot. Auton. Syst.*, vol. 55, no. 3, pp. 191–204, 2007.

[5] W. Dong and J. Farrell, "Cooperative control of multiple nonholonomic mobile agents," *IEEE Trans. Automat. Contr.*, vol. 53, no. 6, pp. 1434–1448, 2008.

[6] R. Ghabcheloo, A. P. Aguiar, A. Pascoal, C. Silvestre, I. Kaminer, and J. Hespanha, "Coordinated path-following in the presence of communication losses and time delays," *SIAM Journal on Control and Optimization*, vol. 48, no. 1, pp. 234–265, 2009.

[7] Y. Kanayama, Y. Kimura, F. Miyazaki, and T. Noguchi, "A stable tracking control method for an autonomous mobile robot," in *Proc. IEEE Int. Conf. Robot. Automat.*, 1990, pp. 384–389.

[8] H. K. Khalil, *Nonlinear Systems*, 2nd ed. Upper Saddle River, NJ: Prentice Hall, 1996.

[9] D. Kostić, S. Adinandra, J. Caarls, N. van de Wouw, and H. Nijmeijer, "Saturated control of time-varying formations and trajectory tracking for unicycle multi-agent systems," in *Proc. IEEE Conf. Dec. and Control*, Dec. 2010, pp. 4054–4059.

[10] F. Mondada and M. Bonani, *E-puck educational robot*, www.e-puck.org, 2007.

[11] N. Moshtagh and A. Jadbabaie, "Distributed geodesic control laws for flocking of nonholonomic agents," *IEEE Trans. Automat. Contr.*, vol. 52, no. 4, pp. 681–686, 2007.

[12] E. Panteley, E. Lefeber, A. Loria, and H. Nijmeijer, "Exponential tracking control of a mobile car using a cascaded approach," in *Proc. IFAC Workshop on Motion Control*, 1998, pp. 221–226.

[13] L. E. Parker, "Multiple mobile robot systems," in *Springer Handbook of Robotics*, B. Siciliano and O. Khatib, Eds. Berlin, Heidelberg: Springer, 2008, pp. 921–941.

[14] A. Rodriguez-Angeles and H. Nijmeijer, "Coordination of two robot manipulators based on position measurements only," *Int. J. Control*, vol. 74, pp. 1311–1323, 2001.

[15] A. Sadowska, T. van den Broek, H. Huijberts, D. Kostić, N. van de Wouw, and H. Nijmeijer, "Virtual structure approach to formation control of nonholonomic unicycle robots," *submitted*, 2011.

[16] O. Sørdalen and O. Egeland, "Exponential stabilization of nonholonomic chained systems," *IEEE Trans. Automat. Contr.*, vol. 40, no. 1, pp. 35–49, 1995.

[17] T. van den Broek, N. van de Wouw, and H. Nijmeijer, "Formation control of unicycle mobile robots: a virtual structure approach," in *Proc. IEEE Conf. Dec. and Control*, 2009, pp. 8328–8333.